FTD-MT-24-160-69

FOREIGN TECHNOLOGY DIVISION

RADAR PROBING OF THE TROPOSPHERE UNDER CLEAR SKY CONDITIONS

by

G. B. Brylev

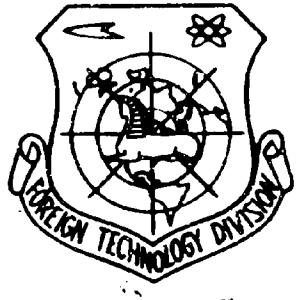

FTD-MT-24-160-69

EDITED MACHINE TRANSLATION

RADAR PROBING OF THE TROPOSPHERE UNDER CLEAR SKY CONDITIONS

By: G. B. Brylev

English pages: 28

Source: Leningrad. Glavnaya Geofizicheskaya Observatoriya. Trudy (Leningrad. Main Geophysical Observatory. Transactions), 1968, No. 231, pp. 38-54.

UR/2531-68-000-231

PREPARED BY:

TRANSLATION DIVISION
FOREIGN TECHNOLOGY DIVISION
WP-AFB, OHIO.

U. S. BOARD ON GEOGRAPHIC NAMES TRANSLITERATION SYSTEM

Block	Italic	Transliteration	Block	Italic	Transliteration
А а	*А а*	A, a	Р р	*Р р*	R, r
Б б	*Б б*	B, b	С с	*С с*	S, s
В в	*В в*	V, v	Т т	*Т т*	T, t
Г г	*Г г*	G, g	У у	*У у*	U, u
Д д	*Д д*	D, d	Ф ф	*Ф ф*	F, f
Е е	*Е е*	Ye, ye; E, e*	Х х	*Х х*	Kh, kh
Ж ж	*Ж ж*	Zh, zh	Ц ц	*Ц ц*	Ts, ts
З з	*З з*	Z, z	Ч ч	*Ч ч*	Ch, ch
И и	*И и*	I, i	Ш ш	*Ш ш*	Sh, sh
Й й	*Й й*	Y, y	Щ щ	*Щ щ*	Shch, shch
К к	*К к*	K, k	Ъ ъ	*Ъ ъ*	"
Л л	*Л л*	L, l	Ы ы	*Ы ы*	Y, y
М м	*М м*	M, m	Ь ь	*Ь ь*	'
Н н	*Н н*	N, n	Э э	*Э э*	E, e
О о	*О о*	O, o	Ю ю	*Ю ю*	Yu, yu
П п	*П п*	P, p	Я я	*Я я*	Ya, ya

* ye initially, after vowels, and after ъ, ь; e elsewhere. When written as ё in Russian, transliterate as yё or ё. The use of diacritical marks is preferred, but such marks may be omitted when expediency dictates.

FOLLOWING ARE THE CORRESPONDING RUSSIAN AND ENGLISH

DESIGNATIONS OF THE TRIGONOMETRIC FUNCTIONS

Russian	English
sin	sin
cos	cos
tg	tan
ctg	cot
sec	sec
cosec	csc
sh	sinh
ch	cosh
th	tanh
cth	coth
sch	sech
csch	csch
arc sin	$\sin^{-1}$
arc cos	$\cos^{-1}$
arc tg	$\tan^{-1}$
arc ctg	$\cot^{-1}$
arc sec	$\sec^{-1}$
arc cosec	$\csc^{-1}$
arc sh	$\sinh^{-1}$
arc ch	$\cosh^{-1}$
arc th	$\tanh^{-1}$
arc cth	$\coth^{-1}$
arc sch	sech^{-1}
arc csch	csch^{-1}
rot	curl
lg	log

RADAR PROBING OF THE TROPOSPHERE UNDER CLEAR SKY CONDITIONS

G. B. Brylev

Several types of radar reflections in the centimeter range in the absence of hydrometeors are now known:

1) discrete-coherent echo;

2) reflections from inversion layers;

3) reflections from layers containing aerosols;

4) reflections from zones of turbulence.

All types are interrelated and can be observed simultaneously, hence the complexity of the problem of radar sounding of the troposphere under clear sky conditions, posed in work [5], is understandable.

In this article we will examine a number of questions connected with sources of reflections of each type and the peculiarities of appearance of such signals.

Discrete-Coherent Echo

The discrete-coherent echo (DKR) is the most widespread type of reflection. The typical properties of the DKR have been studied at various times by various researchers [1, 2, 3, 18, 23, 24, 32], basically at wavelengths from 8.6 mm to 10 cm. Let us enumerate them briefly. Signals have discrete character in time and space. Their duration depends on the time for which a point target is within the radiation pattern of the radar antenna. Reflections are coherent and their envelope has a "mirror" character. On radar nephograms signals are noted in the form of dots, and their size does not exceed the duration of the sounding pulse τ. The amplitudes of reflected signals are practically in dependent of τ. Angle dimensions of the target are less than the width of the radiation pattern θ at any height. Measurement of the width of the backscatter radiation pattern showed that it is $0.5\text{-}1.3^{\circ}$. Concentration of the DKR in a unit volume varies from 10 to 1000 km^{-3}. Effective scattering diameters (EPR) under the assumption of a point target σ (cm^2) have values from 10^{-4} to 10^{-1} cm^2, the most probable being from 10^{-3} to 10^{-2} cm^2 (λ = 3.2 cm).

Recently published results of investigation of the dependence of the effective scattering diameter σ on wavelength [20] λ indicate that $\sigma \sim \lambda^{-4}$. Furthermore, according to data of [4], the depolarized component of the reflected signal P_1 can attain 12-13 dB.

New facts make necessary more detailed consideration of the question of the sources of radar signals from the clear sky.

Hypotheses explaining the DKR, were based on the existence of two different sources of reflection:

1) inhomogeneities of the refractive index of air and sharp gradients of the refractive index,

2) insects and birds.

A total of three models of atmospheric formations can give a reflected coherent signal in the centimeter range. Let us discuss their merits and deficiencies in detail and conformity to the physical properties of the DKR.

Model of the small "thermal." By "thermals," as usual, are understood formations of overheated air, which are detached from the surface layer of air and form closed volumes. The dielectric constant of these volumes differs from that the surrounding air. Under certain conditions such formations under the action of Archimedean forces rise upwards in the form of "bubbles" or streams of overheated air. The following characteristic of "bubbles," expounded in detail in monograph [7], are interesting.

1. Convective movements cause a rise of separate "bubbles" or streams of warmer air.

2. The average distances between "bubbles" are considerably greater than their dimensions.

3. The size of "bubbles" has a wide spectrum — from 10 to 500 m. Their average diameter is 50-100 m.

4. The intensity of "bubbles," or the difference between maximum temperature in a "bubble" and the temperature of the ambient air, is 0.2-0.3°. Maximum intensity is 1.5°.

5. The intensity of rising "bubbles" is practically independent on their dimensions.

6. Their concentration is 750 "bubbles" to the cubic kilometer.

The dielectric constant ε is related to the refractive index n as $\varepsilon = n^2$. The refractive index for centimeter waves is expressed in the form

$$N=(n-1)\cdot 10^6=\frac{77.6}{T}\left(p+\frac{4810}{T}e\right). \qquad (1)$$

Hence change of the refractive index at the thermal-atmosphere boundary is equal to

$$\Delta N = -\frac{77.6}{T^2}\left(p + \frac{9620}{T}e\right)\Delta T + \frac{77.6 \cdot 4810}{T^2}\Delta e. \qquad (2)$$

Up to a height of 3 km for practical purposes the following relationship is valid

$$\Delta N = 0{,}3\Delta p - \Delta T + 5\Delta e. \qquad (3)$$

In formulas (1), (2), and (3) designations are the following: p – pressure, in millibars, T – temperature, in $^{\circ}$K, e – absolute humidity, in millibars, and $\Delta T = T - \overline{T}$, $\Delta e = e - \overline{e}$.

Thus, the examined model constitutes a sphere with radius of 25-35 m, at the boundary of which a sharp change of temperature and humidity takes place. In a number of investigations [1] it was shown that a thin layer with area smaller than the cross-sectional area of the antenna is radiation pattern at the height where reflections are noted reflects. Therefore one may assume that reflection occurs from a microlayer formed as a result of the action of turbulence on the rising "bubble." The value of the reflection factor in power F^2 at the limit with infinitely thin transition zone is expressed by the Fresnel reflection factor. For vertical sounding

$$F^2 = \frac{\Delta n^2}{4} = \frac{\Delta N^2}{4} \cdot 10^{-12}. \qquad (4)$$

Appraisal of Δn made by this formula [3, 20] gave the following values: $10^{-11} \leqslant F \leqslant 10^{-14}$; $10^{-4} \leqslant \Delta n \leqslant 10^{-7}$ for the entire range of values of reflected signals.

Equation (4) characterizes the limiting case. Therefore it is realistic to conceive of the existence of a transition zone in the reflecting layer.

If we assume (Fig. 1) that the profile of the refractive index changes in the transition layer per linear law, ΔN will be expressed by the formula [19, 33]

$$\Delta N = -\frac{\Delta N_{max} \exp\left(\frac{4r}{L}\right)}{1 + \exp\left(\frac{4r}{L}\right)}. \qquad (5)$$

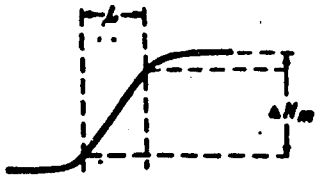

Fig. 1. Change of refractive index in the transition zone.

The value of F^2 decreases rapidly with increase of ratio L/λ, and when $L/\lambda = 0.5$ the reflection factor is 10 dB less the maximum.

Thus, if the horizontal dimension of the reflecting zone does not exceed the radius of the first Fresnel zone and its vertical extent does not exceed the wavelength of the applied radar, the value of EPR σ (cm^2) through irradiated area S^2 is equal to

$$\sigma = F^2 \frac{4\pi S^2}{\lambda^2}. \qquad (6)$$

For permissible values of ΔT and Δe and practically measured Δn it turns out that σ may cause an intensity of echo which for the majority of applied radars should be approximately equal to their threshold sensitivity. The examined model cannot explain the existence of high echo intensities.

Model of the large "thermal." In contrast to the preceding case, the radius of the reflecting volume is increased. The EPR is found by the formula

$$\sigma = F^2 \pi b^2, \qquad (7)$$

where b^2 is the radius of the sphere, which can attain 500 m. For the given model the magnitude of the signal can be one order greater than for the small "thermal." However, in both cases the probability of appearance of very intense variations of the refractive index at a distance of the order of the radar's wavelength should be too high to explain reflected signals by formulas (6) and (7).

The Atlas model. Atlas in work [32] offered one more model: a rising convective "thermal" of hemispheric form, with concavity directed downwards. The "thermal" has a smooth surface with distinct upper boundary, on which exists a sharp gradient of the refractive index. The upper surface reflects and focuses the energy striking it. For the effective cross section of the Atlas "thermal" [19, 32] the following formula is offered:

$$\sigma = \frac{\pi R^2 b^2 F^2}{(R-b)^2}. \qquad (8)$$

where πR^2 – effective scattering diameter of the large metallic plane ($b = \infty$), b – radius of curvature, F^2 – power reflection factor (4) and (5), $g_p = b^2(R-b)^{-2}$ – gain of the hemispheric surface. When $0{,}7 < \frac{R}{b} \leqslant 1{,}3$ $g_p \geqslant 10$. When $R = b$ $\sigma = \infty$.

As can be seen from formula (4), the magnitude of the reflected signal should be directly proportional to the intensity of variations of the refractive index n. In turn the magnitude of variations of n will be the biggest for high mean values of temperature and humidity, when variations of T and e will occur simultaneously, but will have different signs. It is well known [17] that on the average the amplitude of variations of n is increased with growth of the scale of inhomogeneities n should lead to increase of amplitudes of radar signals. Therefore it is possible to expect that good correlation will also exist between the average value of the signal and the gradient of the refractive index, and also humidity. For the purpose of checking this proposition the following experiment was conducted at the GGO field base at Voyeykovo in the summer of 1964. (Method and equipment are described in work [6]). Was selected the layer from 900 to 1450 m, in which the average effective scattering diameter of the DKR $\overline{\sigma}$ over a 5-10-minute interval was determined.

The value of $\overline{\sigma}$ was found from the radar equation for a point target:

$$\frac{P_r}{P_t} = \frac{g^2\lambda^2}{64\pi^3}\frac{\sigma}{R^4},$$

where P_r – received signal, P_t – pulse power of transmitter, g – antenna gain.

The value of $\overline{\sigma}$ (more exactly 10^5 lg $\overline{\sigma}$) was found only in periods of ascent of the probe. From aerological data were calculated the gradient of the refractive index $\frac{dN}{dH}\left(\frac{\text{N unity}}{100\text{ m}}\right)$ and specific humidity q (g/kg). From Figs. 2 and 3 it is clear that the relationship between $\overline{\sigma}$, $\frac{dN}{dH}$, and q is very weak. Such weak relationship exists between $\overline{\sigma}$ and other meteorological parameters if they are noted directly in that layer where the DKR is observed. If we consider the source of reflections to be turbulent-convective inhomogeneities of the refractive index of the above-selected scales, space-time correlation and structural functions of values of reflected signals have to reflect the statistical laws of turbulence. However, as one may see from work [6], such relationship is too unclear. Therefore it was concluded that that from the characteristics of the DKR it is possible only indirectly to judge atmospheric turbulence. (This question is examined in greater detail in article [8]).

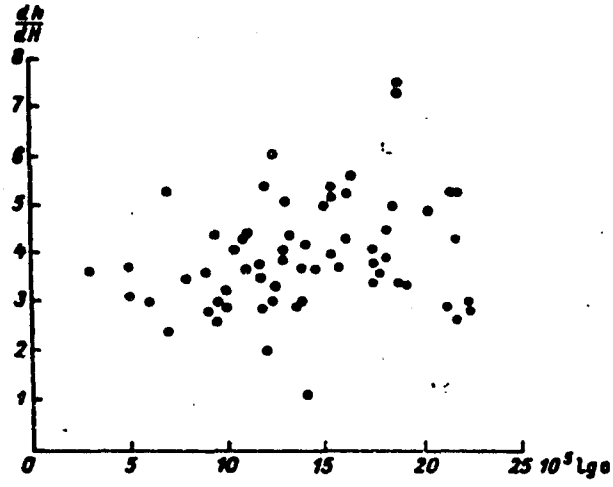

Fig. 2. Relationship between $\frac{dN}{dH}$ and 10^5 lg $\overline{\sigma}$.

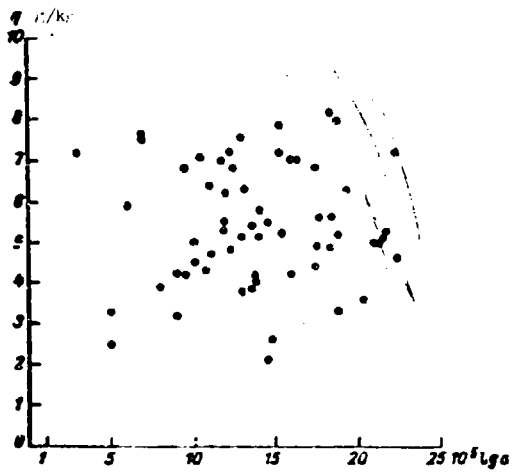

Fig. 5. Relationship between q and $10^5 \lg \bar{\sigma}$.

For all models considered above the presence of a stable boundary between the inhomogeneity of n and the ambient air with thickness of the order of a wavelength is assumed. Turbulent and radiant exchange between the thermal and the ambient air makes the existence of such boundaries with large gradients of meteorological elements improbable. The rate of destruction of the boundary is easy to estimate by solving the heat-conduction equation for a transition layer with thickness $L \approx \lambda$.

Turbulence and radiant exchange make possible the existence of such boundary for hundredths and tenths of a second. And only erosion of the boundary as a result of molecular thermal conduction can explain the duration of signals of up to 10 s with large initial value of $F^2 = 10^{-10}$.

In our reasonings nothing will be changed if we consider that the boundary is determined basically by change of humidity in the transition layer, as follows from formula (3). Diffusion of heat and moisture obeys identical law. Thus, in order to explain the time of existence of the DKR during vertical sounding it is necessary to assume only molecular thermal conduction and a complex mechanism of generation of reflecting zones in the atmosphere by an unknown source.

Thus, models of dielectric inhomogeneities correspond well to macrometeorological conditions of appearance of the DKR [3] and poorly to their physical properties.

Let us list results.

1. Discreteness of echo contradicts the model of the large "thermal."

2. The point nature contradicts the model of the large "thermal" and partially that of the small "thermal."

3. Stability contradicts the Atlas model, since it is difficult to represent a stable surface with diameter of several meters (value of the first Fresnel zone) in the atmosphere.

4. The mirror-like nature is one of weak points of these models. The mirror character of radar echos assumes the presence of a stable boundary with thickness of the order of a wavelength.

5. Coherence. Considering the rate of destruction of reflecting boundaries for these models, we can expect considerable incoherent scattering, which in fact is not noted. Therefore under real conditions the obtaining of coherent signals from such formations is improbable.

6. Lifetime contradicts the models, inasmuch as it is impossible to explain the cause of existence of such gradients for so long a time.

7. Movement of DKR sources corresponds well to models.

8. Data on the concentration of "bubbles" in the atmosphere agree well with experimental data and concentration of DKR.

9. The directed character of radiation agrees well with the Atlas model, does not agree with the model of the large "thermal," and agrees poorly with the model of the small "thermal."

10. The value of the effective scattering diameter is not explained by models of small and large "thermals." The Atlas model explains it with difficulty.

11. Properties of polarization of radar echos do not correspond to models at all.

12. Dependence $\sigma \sim \lambda^{-4}$ cannot be obtained for a single model of the "thermal."

Hence it is obvious that the hypothesis about the reflection of shf energy from fluctuations of the refractive index or sharp gradients of n cannot explain the physical properties and magnitude of signals of the majority of noted DKR's. The probability of appearance of signals due to various sources of scattering will be insignificant, and their amplitude should not exceed 5-10 dB above noise level for the majority of radars on which DKR's were observed.

Insects and birds are also cited as sources of reflections in literature. Signals from birds are several orders higher than those investigated. Thus, according to data of [25], the EPR of a starling is 5.8 cm^2, and that of a sparrow is 3 cm^2. Furthermore, the maximum number of reflections should occur in periods of mass flights of birds, which is not confirmed.

Let us consider the assumption that insects are possible sources of DKR, considering that birds in forming the DKR are sharply distinguished by the magnitude of the reflected signals.

1. From this point of view there naturally is observed seasonal variation of radar echos.

2. It is not difficult to explain the connection between air temperature, its humidity, and the concentration of sources of DKR in the atmosphere. It is known that high temperature and high humidity favor the appearance of convective movements, i.e., conditions are created here for the ascent of insects to high altitudes. Furthermore, these conditions promote maximum insect activity:

a) in particular, for the Locust general activity is increased in humid atmosphere and drops in dry [9, p. 286];

b) flight of Melontha hippoca stani is possible, for example, at temperatures not lower than 7 or 5-9°C [9, p. 280].

The fact that threshold values of temperature and humidity, for which DKR is absent, are easily explained by the fact that insect activity ceases when T and e lower than these values is very significant [9, p. 280].

3. In connection with explanation of the concentration of DKR and maximum height of their appearance, data from direct observations of insects at such heights is interesting. Insects are encountered to a height of 2000-4000 m, and possibly higher [10, p. 125]. In this book it is indicated that according to certain data, in a column of air with a base of 1 square mile and height of 4285 m (starting with 15 m above the earth), on the average, for a whole year up to 25,000,000 insects were found [ibid, p. 125].

All the aforementioned indicates the conformity of meteorological conditions of appearance of DKR to the hypothesis on insects as sources of radar echos.

It is known that insects are made up of approximately 60% water (hemolymph). However, the covering of insects (cuticle) is low in water and mineral salts — 1-3% [9, p. 7] and constitutes a layer with thickness of not over 10 microns, containing chitin, albumin substances, and certain fatty acids.

Since the dielectric constant of these substances is much lower than that of water, a layer with thickness of 10 microns can be freely disregarded, and it can be considered that the dielectric constant of insects is equal to that of water in the centimeter range of wavelengths. Measurements taken in [20] show that EPR can vary for different varieties of insects from $5 \cdot 10^{-2}$ to 0.5 cm^2.

From tables of [21], analogously to [20], a graph of the dependence of σ on λ (Fig. 4) was plotted on the assumption that the sources of the DKR are water spheres with diameters of 0.15, 0.40, and 0.80 cm.

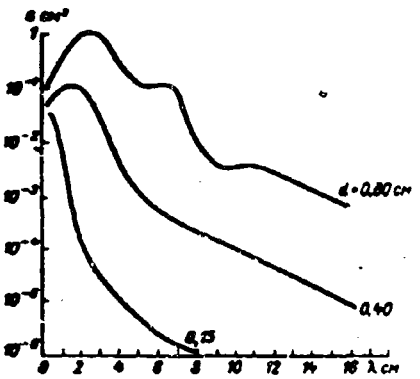

Fig. 4. Dependence of σ of water spheres of various diameter on wavelength.

Obtaining the practical dependence of σ on λ is simply only in the region of Rayleigh scattering. The varying character of EPR with increase of dimensions of reflecting particles (region of Mi scattering) and the various thresholds of detection at selected wavelengths and error in determination of σ create considerable difficulties in determination of function $\sigma(\lambda)$. For example, if the maximum absolute error in measurement of σ = ±2.5 dB, then for λ_1 = 0.86 cm and λ_2 = 3.2 cm (Fig. 5) comparison is possible to a diameter of 0.4 cm. On the basis of the radar equation for point targets values of $\sigma(\lambda_1)/\sigma(\lambda_2)$ and δ_1/δ_2 are interrelated as:

$$\frac{\sigma(\lambda_1)}{\sigma(\lambda_2)} = \frac{A_1^2 \lambda_1^2 P_{t_1} P_{r\min_1} \delta_1}{A_2^2 \lambda_2^2 P_{t_2} P_{r\min_2} \delta_2}, \qquad (9)$$

where A_1 and A_2 – effective areas of antennas at wavelengths λ_1 and λ_2; P_{t_1} and P_{t_2} – pulse powers of transmitters; $P_{r\,\min_1}$ and $P_{r\,\min_2}$ determine minimum detectable signal for both stations; δ_1 and δ_2 – ratios of minimum powers of echos detectable at both wavelengths.

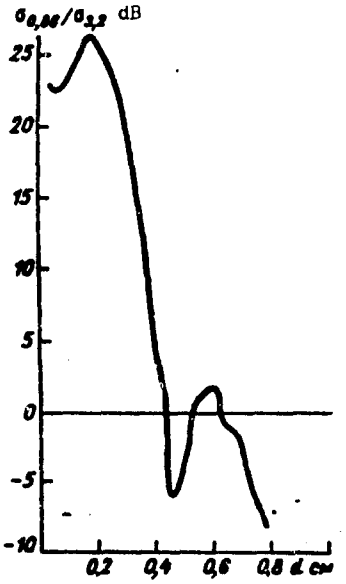

Fig. 5. Ratio $\sigma_{0.86}/\sigma_{3.2}$ in decibels, depending upon diameter of water sphere.

In August 1961, at TsAO such measurements were made at $\lambda = 16$ cm and $\lambda = 3.2$ cm. Deviations of ratio $\sigma(\lambda_1)/\sigma(\lambda_2)$ from unity did not exceed errors of measurements. Hence author [1] could not draw a correct conclusion concerning the dependence of σ on λ. This measurement corresponds to sizes of insects of more than 1.6 cm [31].

Now we will cover briefly the conformity of this model to the physical properties of the DKR.

1. Discreteness and point nature are achieved automatically.

2. With this concentration of sources, which is observed (i.e., $l \gg \lambda$, where l is the distance between targets), the properties of coherence, "mirror-like nature," and stability prevail. Let us note that superposition of a periodic component on the envelope of the radar echo (a fact that is inexplicable from the stand point of dielectric inhomogeneities) is easily explained by the rotation of an insect having the form of an ellipsoid around its small axis. This leads to modulation of the reflected signal.

3. Movement of sources of DKR is caused by the fact that insects are tossed to heights by air currents and are carried with them.

4. Reflection from insects does not meet with objections during determination of signal and allows large depolarization factors.

5. The effects of the component of the speed of shift with respect to wind speed are easily explained [1, 21].

Thus, the conclusion can be made that the hypothesis on insects as sources of DKR completely satisfies both the meteorological and physical properties of radar echos and explains the absolute majority of reflections. Such opinion is held also by the authors of works [4, 20, 21].

Reflections Connected with Inversions

Reliable radar detection of inversion layers in the atmosphere is possible. Much information indicates that [18, 30]. However, the mechanism explaining reflection remains debatable.

In inversion layers sharp changes of speed and direction of wind and also of humidity are observed. From formulas (1) and (2) it is clear that temperature rise and fall of humidity are especially favorable for formation of strong inhomogeneities of the refractive index. Inversions are also retarding layers for propagation of impurities in the atmosphere. Under inversions in free atmosphere the concentration of aerosols, dust particles, and micro-organisms is considerably greater than in other layers. Finally, under inversions small-scale turbulence appears, which can give reflected signals.

Thus, the region of an inversion can be detected by radar as:

1) a flat layer with sharp gradient of refractive index;

2) a layer with concentration of aerosol particles;

3) a layer of finite vertical extent, enveloped by turbulent variations of refractive index.

The horizontal extent of inversion layers can attain tens of kilometers. The vertical extent of an inversion can vary widely. For example, from 100 recordings of inversions made in clear weather from April through November for several years [29], the average vertical extent of inversions was approximately 100 m, and in 25% of the cases it was less than 40 m, and less than 8 m in 10%.

It is necessary to note that under inversion layers there is raised concentration of the DKR. With low wind speed and sufficiently high concentration of DKR an echo of laminar type can also be obtained. In many cases DKR's promote reliable detection of inversions even in radar with comparatively low potential.

Let us consider the contribution to the magnitude of the reflected signal made by each of the possible sources of scattering.

1. Reflection from a solid layer. The radar equation for an infinitely thin extended layer is recorded in the following form:

$$\frac{P_r}{P_i} = \frac{g^2\lambda^2}{64\pi^2}\frac{|F|^2}{R^2}. \qquad (10)$$

The magnitude of the coherent signal from the layer Δn is determined by formula (2). Let us select the parameters of the radar in such a way that for a signal-to-noise ratio of 1 the reflection factor is related to distance R to the reflecting layer by the expression

$$|F| = 10^{-12}R. \qquad (11)$$

When $R = 10^3$ м $|F| = 10^{-9}$; when $R = 2\cdot 10^3$ м $|F| = 2\cdot 10^{-9}$.

If it is considered that reflection is produced by a region including several Fresnel zones, the values of $\Delta N = 2 \cdot 10^{-3} N$ unity, and here $\Delta T = 0.048^{\circ}C$ and $\Delta e = 0.05$ mbar at a distance of $\lambda/4$. Inasmuch as real signals are 1-2 orders greater than those selected and $|F|^2$ decreases sharply with increase of thickness of the layer, Δe and ΔT will increase by 2-3 orders. As in the case with the DKR, it is difficult to assume the existence of such large gradients in a layer with depth of from one to several centimeters. As was noted above, the selected mechanism of reflection from layers with sharp gradient of refractive index seems more convincing from the meteorological stand point with increase of wavelength.

2. Inversions with raised concentration of aerosol under them. With dimensions of aerosols much smaller than the wavelength of the applied radar the refractive index of air can be replaced by the refractive index of a mixture of two gases – air and aerosol.

For calculation of ΔN in the 3-centimeter range the following expression is offered in work [26]:

$$\Delta N = 1{,}5\left(\frac{n_a^2 - 1}{n_a^2 + 2}\right)\frac{C}{\rho}, \qquad (12)$$

where n_a – refractive index of aerosols, ρ – density of weighed particles (g/cm^3), C – concentration by weight of aerosols in air ($\mu g/cm^3$).

Equation (12) is valid for $C \leq 5$ $\mu g/cm^3$.

Table 1 contains data pertaining to different impurities in the atmosphere [26].

Calculation made according to formula (12) under the assumption of coherent scattering and with selected parameters of radar (11) shows that weak signals can be noted at a distance of 1 km only for carbonate aerosols. Furthermore, the requirement on depth of the reflecting zone, equal to $\lambda/4$, is very strict, and an increase of depth of the zone considerably reduces the already small value of the

reflected signal. Therefore increasing the potential of the radar in the centimeter range leads to growth of the "dead" zone as a result of increased intensity of reflections from local objects, caused by the side lobes. This can neutralize detection of inversion layers for a given mechanism of scattering.

Table 1. Physical characteristics of aerosols.

Name of impurities	ρ g/cm^3	c μg/cm^3	$\frac{n_a^2-1}{n_a^2+2}$
Aerosols	1,032—7,31	2—5	0,3—10^{-12}
Quartz	2,6		0,3
dust		10^{-2}—$5\cdot10^{-5}$	
dust storms		0,5—9	
ejections from factory smokestacks.		10—80	
Carbonat aerosols	2	1	≈ 1
Aerial bacteria		$5\cdot10^{-11}$	≈ 1
Pollen	0,5	$6\cdot10^{-8}$	0,4—0,9
Ejections from blast furnaces and foundaries		0,4—10	≈ 1
Micrometeorites		5	≈ 1

At Voyekovo during summer observations reflections of laminar type were recorded on radar nephograms during visual observations of city smoke at high altitudes. Recording of amplitudes of echoes of such type shows that in them, in addition to the DKR, there is a constant signal component, not above the noise by more than 3-5 dB and having coherent character. Such cases were recorded during westward shift and with low wind speed, when the city smoke was due to the proximity of the industrial enterprises of Leningrad. In monograph [12] are given data on the ground concentration of aerosols at Voyekovo. In particular, the conclusion is drawn that with westerly winds the daytime concentration of atmospheric aerosols is 5 times more than with northerly winds.

It is obvious that when $C \geq 5$ μg/cm^3 for calculation of reflected signals it is necessary to use the radar equation for volume scattering. In this case of particles of aerosol will be Rayleigh scatters with refractive index of n_a. The effective diameter of one particle σ

$$\sigma(r_a) = \frac{64\pi^5 r_a^6}{\lambda^4}\left(\frac{n_a^2-1}{n_a^2+2}\right)^2. \qquad (13)$$

The effective scattering diameter of a unit volume η (cm^{-1})

$$\eta = \int_0^\infty n(r_a)\sigma(r_a)dr_a. \qquad (14)$$

where $n(r_a)$ is distribution density of particles by size.

The maximum size of dust motes, in accordance with that generally accepted [12], is 100 μ. The Stokes rate of settling of particles with radius r_a = 100 μ in calm atmosphere is approximately 0.75 m/s, while with radius r_a = 10 μ it is 100 times less. Hence it is improbable that particles with radius r_a = 100 μ could be at a height of 1 km and above.

The distribution of "giganic" aerosols by size can be represented by expression [13]

$$N_{r_a > r_0} = \frac{A}{r_0^3}. \qquad (15)$$

We will consider that the distribution density for aerosols, starting from r_0 = 4 μ, is described analogously to the distribution for big drops in clouds [14] by an expression of form

$$n(r_a) = (\varkappa - 1)\frac{N_i}{r_0}\left(\frac{r_0}{r_a}\right)^\varkappa. \qquad (15a)$$

Here N_i is average particle density, the radius of which exceeds 4 μ.

According to data of [13], in summer conditions at a height of 1 km $N_i = (3\text{-}4) \times 10^{-2}$ particles/cm^3.

Substituting (15a) in formula (14) and integrating from r_0 to r_{max} with $\varkappa = 4$, we obtain η (cm^{-1})

$$\eta = \frac{64\pi^5}{\lambda^4}\left(\frac{n_a^2 - 1}{n_a^2 + 2}\right) N_i r_0^3 (r_{a_{max}}^3 - r_0^3). \qquad (16)$$

Let us calculate the graph $\eta(r_{a_{max}})$ for various values of N_i, assuming that formula (15a) is valid for $r_{a_{max}} > 12\ \mu$. (Calculation is carried out for carbonate particles, Fig. 6).

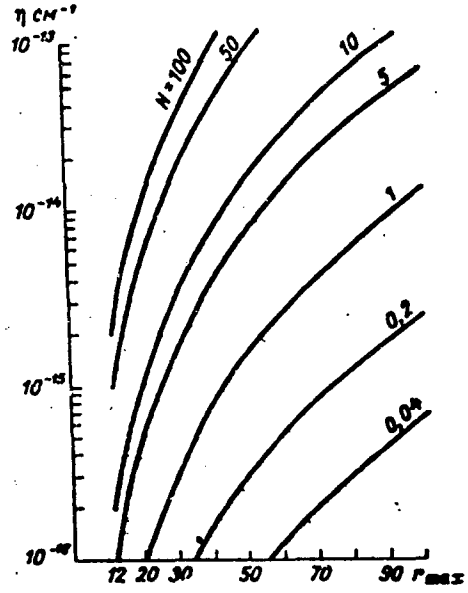

Fig. 6. Dependence of $\eta(cm^{-1})$ on concentration of "gigantic" aerosols.

We determine η_{min} from a radar equation of form

$$P_r = \frac{P_i g^2 \lambda^2 \theta^2 h}{512\pi^2} \frac{\eta}{R^2}. \qquad (17)$$

Expression $\frac{P_i g^2 \lambda^2 \theta^2 h}{512\pi^2}$ we designate by Π, then

$$\eta_{min} = \frac{P_{r\,min} R^2}{\Pi}. \qquad (17a)$$

At distance R = 1 km for carbonates, with the selected parameters of the radar [formula (11)], η_{min} is changed from $1.41 \cdot 10^{-16}$ to 3.44×10^{-15} cm^{-1}. On the graph (Fig. 6) are revealed layers with concentration exceeding the usual by 25-100 times. Tentative results were obtained under the condition of total filling of the pulse volume. In case of incomplete filling the value of η is increased somewhat.

Thus, radar detection of inversions due to the various sources of scattering is possible to low heights (1-2 km) with optimum parameters of radar and shown heights of propagation of impurities in the atmosphere.

Layers of smoke in the free atmosphere will be better observed with decrease of wavelength, in particular at millimeter wavelengths. Calculation for dust shows that the concentration of dust (quartz) must be two orders higher in order for the radar to detect it. The character of the reflected signal must be incoherent, analogous to the signal from clouds and precipitation.

Radar Detection of Turbulence

Radar detection of turbulence in clear sky, and also of the tropopause, has great value for the problem of propagation of radio waves and aviation. The possibility of such detection is based on the theory of scattering of radio waves in turbulent inhomogeneities of the refractive index of air [17]. There recently appeared a number of theoretical and experimental investigations [20, 27, 28, 30] in which this question is illuminated in reference to radar. Let us mention briefly the basic conclusions of these works.

In scattering at a defined angle φ only a small group of spectral components of turbulence, forming spatial diffraction gratings of fixed period l

$$l = \frac{\lambda}{2 \sin \frac{\varphi}{2}}. \qquad (18)$$

In the region of isotropic turbulence, where the -5/3 law is met, the value of the effective scattering diameter $\eta(cm^{-1})$ is proportional to the intensity of inhomogeneities of the refractive index, the scales of which satisfy (18) [17],

$$\eta = \frac{128\pi^2}{\lambda^2}\Phi_n\left(\frac{4\pi}{\lambda}\right), \tag{19}$$

where $\frac{4\pi}{\lambda} = k$ – wave number, $\Phi_n(k)$ – three-dimensional spectrum of variations of refractive index within the region of turbulent mixing,

$$\Phi_n(k) = 0{,}033C_n^2 k^{-11/3} \text{ for } K_0 < k < k_0,$$
$$\Phi_n(k) = 0 \text{ for } k > k_0. \tag{20}$$

The -5/3 law is valid within limits of the "inertial" interval, limited by the external L_0 and internal l_0 scales of turbulence, which are determined as follows. The external scale L_0 in the case of set turbulence is expressed through the coefficient of turbulent diffusion k' and the vertical gradient of average wind speed β

$$L_0 = \left(\frac{k'}{\beta}\right)^{0.5}.$$

The internal scale of turbulence is connected with the limiting (Kolmogorov) microscale l_m through the kinematic viscosity of air ν, the universal dimensionless constant a, and dissipation of turbulent energy ε

$$l_0 = 2{,}72a^{3/4} l_m = 2{,}72a^{3/4}\left(\frac{\nu^3}{\varepsilon}\right)^{1/4}. \tag{21}$$

Limits of change of l_m from a few millimeters in the surface layer to several centimeters in the troposphere (2.3 cm at a height of 10 km [20])

$$l_m \approx \frac{L_0}{Re^{3/4}}, \tag{22}$$

i.e., the limiting microscale decreases with increase of turbulence. When $l < l_m$ the -5/3 law is violated and there is rapid dissipation, caused by molecular viscosity.

The intensity of small-scale inhomogeneities of the refractive index is characterized by the structural constant C_n^2 ($cm^{-2/3}$), which is connected with the average wind profile, temperature, and humidity,

$$C_n^2 = a^2 L_0^{4/3} M^2, \tag{23}$$

where M is the gradient of the average potential index of refraction (mixing occurs under adiabatic conditions). Another determination of C_n^2, connected not with M, but with the mean square deviations of the refractive index $\overline{(\Delta n)^2}$ in direction of sounding, is given in work [20]

$$\overline{(\Delta n)^2} = 0{,}19 \cdot L_0^{4/3} C_n^2. \tag{24}$$

The value of C_n^2 can vary from 10^{-12} $cm^{-2/3}$ (on the basis of the model of face convection [16]) to 10^{-17} $cm^{-2/3}$ [17]. According to data of [20, 22], in the troposphere the maximum value of $C_n^2 = 10^{-14}$ $cm^{-2/3}$, and in the region of the tropopause $C_n^2 \approx 10^{-16}$ $cm^{-2/3}$. The value of C_n^2 decreases with height and has annual variations with maximum in July.

From the equations it is clear that the intensity of inhomogeneities depends simultaneously on the mean value of the refractive index and the structure of turbulence. Values of C_n^2 and M in the troposphere can vary within limits of three orders of magnitude. From formula (19), taking into account (20) and (24), the effective scattering diameter will be expressed as follows:

$$\eta = 0{,}39 C_n^2 \lambda^{-1/3} = 0{,}61 \overline{(\Delta n)^2} K_0^{4/3} \lambda^{-1/3}. \tag{25}$$

In selecting optimum wavelength and parameters of radar for detection of turbulence it is necessary to consider a number of factors:

1) the relationship between η and λ ($\eta \sim \lambda^{-1/3}$);

2) the relationship between l_m and l is equal to 0.5λ, inasmuch as $\Phi_n(k) \to 0$ when $\eta > k_m$. Conclusions drawn in [17] are extended in [20, 22] to that section of the spectrum where the -5/3 law is not satisfied. In particular, when $\lambda = 0.5\, l_m$, it is possible to expect a decrease in η of 10 times;

3) The intensity of turbulence and the potential of the radar with fulfillment of the condition of volume scattering

$$\overline{(\Delta n)^2} \approx C_n^2 > \Pi R^{-4/3}.$$

If in the lower troposphere, from 1 to 3-4 km, for large values of the average gradient of the refractive index a very low dynamic factor can cause great variations of n, in the upper troposphere, including the tropopause, η is more strictly related to changes of temperature and dynamic factors. In the region of temperature inversions it is possible to expect [30, 22] changes in the nature of the turbulent spectrum as a result of the influence of Archimedean forces. Furthermore, for inversions of the free atmosphere the external scale L_0 is probably of the same order as the vertical extent of the inversion [20];

4) spatial dimensions of the zones of turbulence in clear sky, affecting the degree of filling of the reflecting volume. Reflecting volume V, when approximated by a cylinder through the duration of the sounding pulse τ and width of antenna radiation pattern θ at distance R, is equal to

$$V = \frac{\pi}{8} R^2 \theta^2 c\tau. \qquad (26)$$

In particular, for an antenna in the form of a paraboloid of revolution with diameter D, and θ in radians,

$$\theta = \frac{0{,}39 \lambda}{D}. \qquad (27)$$

Inasmuch as an infinitely large antenna cannot be built, and with increase of wavelength the width of the directivity pattern increases, an important limitation arises.

Dimensions of zones with sharp gradient of refractive index are given in work [29]. The most important conclusion which can be drawn from this is the following: radar is able to detect thin inversion layers (less than 10 m), which the ordinary radioprobe cannot discern.

After analysis of experimental data the authors of [20, 22] came to conclusion that the optimum wavelength must be between 5 and 10 cm. The basic drawback to the wavelength is simultaneous detection of clouds of the upper and middle strata and zones of turbulence. In order to separate signals from clouds and zones of turbulence it is apparently necessary to use equipment for spectral analysis, so that from the spectral characteristics of reflected signals these phenomena can be separated. With increase of wavelength Rayleigh scattering for identical potentials of radars produces signals that are considerably lower (to 40 dB) than proposed for detection of zones of turbulence. From this standpoint the optimum wavelength should be of the order of 80 cm. The potentials of radars and the widths of their radiation patterns impose considerable limitations on detection range of zones of turbulence in clear sky. In the experiments of [20] this range did not exceed 50 km.

The value of η_{min} can be determined by means of the radar equation offered by the authors of [22]:

$$\eta_{min} = \frac{P_{min} \cdot 8\pi R^2}{0{,}445 P_t \psi A_p \lambda \cdot 10^{-13}}, \qquad (28)$$

where A_p – antenna aperature, ψ – coefficient considering filling of beam, β – coefficient for losses in the waveguide channel of the receiver.

In accordance with the value of the effective scattering diameter η at λ = 10.7 cm and λ = 71.5 cm and relationship (25) in work [20] structural constant C_n^2 was determined by the following formula:

$$C_n^2 = 2{,}56\eta\lambda^{1/3}. \qquad (29)$$

In the tropopause region the mean value of $C_n^2 = 3.5 \cdot 10^{-16}$ cm$^{-2/3}$. Here the probability of detection of turbulence at a wavelength of 3.2 cm is much less than at 10.7 and 71.5 cm. On the one hand, as assumed in [20], this is caused by lower sensitivity and power of the applied radar, and on the other by the relationship between wavelength and limiting microscale ($l_m > \lambda/2 = 1.6$ cm).

In order to check the probability of detection of zones of turbulence in clear sky, from April through September 1966 at the GGO observations were made on the 3-cm channel of a weather radar with storage unit of the TsAO system (with this equipment a signal from the tropopause region had already once been obtained [15]). With vertical sounding in periods of ascent of the probe and with cloudless sky in the area of observation for 43 days, 67 series of observations were run. A signal from a height of 11.8 km, coinciding with the height of the tropopause according to aerological soundings, was noted only on one day – 20 June 1966 (Fig. 7). The magnitude of the signal was 142 dBW; $\eta = 3 \cdot 10^{-15}$ cm^{-1}. In Fig. 7 the second signal at 15 km is a reflection from a local object due to the antenna's side lobes. From equations (28) and (29) the value of $C_n^2 \approx 10^{-14}$ cm$^{-2/3}$; according to [22], this is the maximum value which can be attained in troposphere.

Thus, using a wavelength of 3.2 cm with a given potential of the radar, it is possible to detect the tropopause only in exceptional cases. All the above-stated theory is in need of thorough experimental check. Its main problems will be questions of potentials and wavelength of the radar equipment and clarification of the actual relationship between range and intensity of detected turbulence.

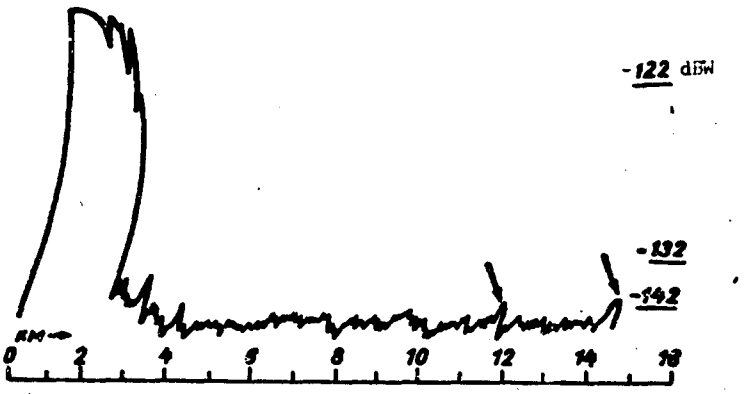

Fig. 7. Recording of radar signal from tropopause. 20 June 1966, 1018 hours.

Conclusions

Consideration of principles and possible sources of radar reflections in cloudless sky shows that radar sounding can give information about heights of inversion layers and zones of turbulence. This is necessary for the theory and practice of propagation of radio waves as a result of scattering in turbulent inhomogeneities of the refractive index of air, for aviation, and for meteorological investigations of the troposphere.

The probability of obtaining such information, its quality, and its detail will in great measure be determined by wavelength and other parameters of the radar equipment used. Depending upon season, altitude, and the character of reflected signals, the cause of their appearance will be different.

Development of the questions posed requires thorough experimental check and the gathering of statistical data for clarification of the representativeness and reliability of data from radar soundings.

Bibliography

1. Chernikov A. A. Radiolokatsionnyye issledovaniya otrazheniy ot yasnogo neba. (Radar investigations of reflections from clear sky.) Tr. TsAO, vyp. 48, 1963.

2. Kostarev V. V., Gorelik A. G. Radioekho nekotorykh nevidimykh ob'ektov troposfery. (Echoes from certain invisible objects of the troposphere.) DAN SSSR, t. 125, No 1, Izd. AN SSSR, M., 1959.

3. Brylev G. B., Sal'man Ye. M. Radioekho dielektricheskikh neodnorodnostey termicheskogo kharaktera. (Echoes from dielectric inhomogeneities of thermal character.) Tr. GGO, vyp. 121, 1961.

4. Chernikov A. A., Shupyatskiy A. B. Polyarizatsionnyye kharakteristiki radiolokatsionnykh otrazheniy ot yasnogo neba. (Polarization characteristics of radar reflections from clear sky.) Izv. AN SSSR, seriya "Fizika atmosfery i okeana", t. 3, No 2, 1967.

5. Brylev G. B., Vasil'chenko I. V., Selitskaya V. I., Fedorov A. A. Sovmestnyye radiolokatsionnyye i aerologicheskiye nablyudeniya v nizhnem 1.5-km sloye atmosfery (Joint radar and aerological observations in the lower 1.5-km layer of the atmosphere.) Tr. GGO, vyp. 173, 1965.

6. Brylev G. B., Fedorov A. A. Prostranstvenno-vremennyye kharakteristiki radiolokatsionnykh otrazheniy ot yasnogo neba. (Space-time characteristics of radar reflections from clear sky.) Tr. GGO, vyp. 217, 1967.

7. Bul'fson N. I. Issledovaniye konvektivnykh dvizheniy v svobodnoy atmosfere. (Investigation of convective movement in the free atmosphere.) Izd. AN SSSR, 1961.

8. Vrylev G. B., Vasil'chenko I. V., Selitskaya V. I., Fedorov A. A. Osobennosti raspredeleniya diskretno-kogerentnogo radioekho s vysotoy i ikh svyaz' s dannymi aerologicheskogo zondirovaniya. (Peculiarities of distribution of discrete-coherent echoes with height and their relationship to data from aerological soundings.) Sm. nastoyashchiy sbornik.

9. Shoven R. Fiziologiya nasekomykh. (Insect physiology.) IL, M., 1953.

10. Ioganzen B. G. Osnovy ekologii. (Fundamentals of ecology.) Tomsk, 1959.

11. Pringl Dzh. Polet nasekomykh. (Flight of insects.) IL, M., 1963.

12. Selezneva Ye. S. Atmosfernyye aerozoli. (Atmospheric aerosols.) Gidrometizdat, L., 1966.

13. Laktionov A. G. Rezul'taty issledovaniya estestvennykh aerozoley nad razlichnymi rayonami SSSR. (Results of investigation of natural aerosols over different regions of the USSR.) Izv. AN SSSR, ser. geofiz., No 4, 1960.

14. Borovikov A. M., Mazin I. P., Nevzorov A. N. Nekotoryye zakonomernosti raspredeleniya krupnykh chastits v oblakakh razlichnykh form. (Certain regularities of distribution of large particles in clouds of different forms.) Izv. AN SSSR, ser. "Fizika atmosfery i okeana", t. 1, No 3, 1965.

15. Zhupakhin K. S. Nekotoryye rezul'taty radiolokatsionnykh zondirovaniy troposfery i tropopauzy. (Certain results of radar soundings of the troposphere and tropopause.) Tr. GGO. vyp. 177, 1965.

16. Gurvich A. S., Meleshkin B. N. Ob opredelenii vnutrennego masshtaba turbulentnosti po fluktuatsiyam intensivnosti sveta. (Determination of the internal scale of turbulence in accordance with fluctuations of light intensity.) Izv. AN SSSR, ser. "Fizika atmosfery i okeana", t. II, No 7, 1966.

17. Tatarskiy V. I. Teoriya fluktuatsionnykh yavleniy pri rasprostranenii voln v turbulentnoy atmosfere. (The theory of fluctuating phenomena during the propagation of waves in turbulent atmosphere.) Izd. AN SSSR, M., 1959

18. Atlas D. Advances in Radar Meteorology. Advances in Geophysics, v. 10, Academic Press, New York, 1964.
19. Atlas D. Radar studies of meteprological "angel" echoes. Journal of Atmospheric and Terrestrial Physics, v. 15, No. 3/4, 1959.
20. Hardy K. R., Atlas D., Glover K. M. Multiwavelength backscatter from the clear atmosphere. Journal of Geophysical Research, v. 71, No. 6, 1966.
21. Browning K. A., Atlas D. Some clear-air dot angels. Journal of Atmospheric Sciences, v. 23, No. 1, 1966.
22. Atlas D., Hardy K., Naito K. Optimizing the radar detection of clear-air turbulence. Journal of Applied Meteorology, v. 5, No. 4, 1966.
23. Geotis S. G. On sea breeze "angels". Proc. World Conference on Radio Meteorology. Boulder, Colo, Boston, 1964.
24. Jones R. F. Radar echoes from inhomogenities. Q. J. Roy. Met. Soc., v. 84, 1958.
25. Houghton E. W. Detection, recognition and identification of birds on radar. World Conference on Radio Meteorology, Boulder, Colo. Boston, 1964.
26. Hajovsky R. G., La Grone A. N. The effects of aerosoles in the atmosphere on the propagation of microwave signals. Journal of Atmosphere and Terrestrial Physics, v. 28, No. 4, 1966.
27. Wagner R. J., Conant L. C. Radar observations of clear atmosphere between 10,000 and 30,000 feet. Proc. 10th Weather Radar Confirence. Am. Met. Soc., Boston, 1963.
28. Smith P. L., Rogers R. R. On the possibility of radar detection of clear-air turbulence. Proc. 10th Weather Radar Conference. Am. Met. Soc., Boston, 1963.
29. Lane J. A. Some investigations of the structure of elevated layers in the troposphere. Journal of Atmospheric and Terrestrial Phisics, v. 27, No. 9, 1965.
30. Saxton J. A., Lane J. A., Meadows R. W., Mathews R. A. Layers structure of the troposphere. Proc. IEE, No. 3, 1964.
31. Stephens J. J. Radar cross-sections for water and ice spheres. Journal of Meteorology, v. 18, 1961.
32. Atlas D. "Angels" in focus. Rroc. World Conference on Radio Meteorolcgy. Boulder, Colo, Boston, 1964.

DATA HANDLING PAGE

61-ACCESSION NO. 62-DOCUMENT LOC	20-TOPIC TAGS
TT9501306	atmospheric turbulence, meteorologic radar, radar echo, troposphere, aerosol, temperature inversion, clear air turbulence
64-TITLE RADAR PROBING OF THE TROPHOSPHERE UNDER CLEAR SKY CONDITIONS	
47-SUBJECT AREA 04, 17	

12-AUTHOR CO-AUTHORS	10-DATE OF INFO
BRYLEV, G. B.	-----68
43-SOURCE LENINGRAD. GLAVNAYA GEOFIZICHESKAYA OBSERVATORIYA. TRUDY (RUSSIAN)	FTD- MT-24-160-69 / 69-PROJECT NO 60502

63-SECURITY AND DOWNGRADING INFORMATION	66-CONTROL MARKINGS	97-HEADER CLASN
UNCL. 0	NONE	UNCL

76-REEL FRAME NO	77-SUPERSEDES	78-CHANGES	60-GEOGRAPHICAL AREA	NO OF PAGES
1889 2109			UR	28
CONTRACT NO.	**X REF ACC. NO.**	**PUBLISHING DATE**	**TYPE PRODUCT**	**REVISION FREQ**
	65-AT8020176	94-	TRANSLATION	NONE

STEP NO.	ACCESSION NO.
02-UR/2531/68/000/231/0038/0054	

ABSTRACT

(U) The author discusses the nature and the origins of radar echoes in clear air in the absence of hydrometeors. Four different types are defined: 1) discrete-coherent echo, 2) reflections from inversion layers, 3) reflections from layers containing aerosols, 4) reflections from regions of turbulence. The first type of radar return can be explained either by innomogeneities in the refractive index of the air or by the presence of insects or birds. The author comes to the conclusion that models based on variations in the refractive index are inconsistent with some important aspects of this phenomenon. On the other hand, eliminating birds as the source of such echoes because the magnitudes of signals due to reflections from birds are several orders of magnitude higher than those under consideration, the hypothesis that insects are the source of the discrete-coherent echoes fully satisfies the meteorological and physical properties of such signals. Reflections from the inversion layers are due to abrupt changes in the refractive index of air caused by the local temperature differences as well as to the presence of aerosols. The latter source is extensively discussed. Orig. art. has: 7 figures, 1 table, and 29 formulas.